

Original Research

The Structural Changes of Frontal Subregions and Their Correlations with Cognitive Impairment in Patients with Alzheimer's Disease

Cailing Shi^{1,†}, Hao Deng^{1,†}, Xia Deng¹, Dingcai Rao¹, Wenjun Yue^{1,*}¹Department of Radiology, Affiliated Hospital of North Sichuan Medical College, 637000 Nanchong, Sichuan, China*Correspondence: ywj820@163.com (Wenjun Yue)

†These authors contributed equally.

Academic Editor: Gernot Riedel

Submitted: 16 November 2022 Revised: 9 December 2022 Accepted: 15 December 2022 Published: 20 July 2023

Abstract

Background: The frontal lobe is affected by Alzheimer's disease (AD) and mild cognitive impairment (MCI). However, we still lack sufficient understanding of subregion atrophy in the frontal cortex, and the relationship between subregions volume and cognitive decline in AD or MCI remains unclear. **Methods:** This study enrolled 434 participants from the Alzheimer's Disease Neuroimaging Initiative (ADNI), including 150 cognitively normals (CN), 187 subjects with MCI, and 97 patients with AD. The gray matter of frontal regions and subregions was divided based on the BNA-246 atlas and its volume was measured by voxel-based morphometry (VBM). Analysis of covariance was performed to compare the differences in frontal regions and subregions volume. Then, receiver operating characteristic (ROC) curve and the area under the curve (AUC) were used to analyze the discriminative ability of subregion volume to distinguish the three groups. In addition, we investigated the association of subregion volume with Mini-Mental State Examination (MMSE) score and Alzheimer's Disease Assessment Scale-Cognitive Behavior section (ADAS-cog) scores with age, gender, education, and the estimated total intracranial volume (eTIV) as covariates. **Results:** In addition to the regions of frontal lobe atrophy found in previous studies, atrophy of the precentral gyrus (PrG) and some of its subregions were found in MCI. The volume of the right dorsal area 9/46 (MFG_7_1) was the best index to differentiate AD from CN, with an AUC value of 0.7. Moreover, we found that some subregions are associated with cognition in patients with MCI and AD. **Conclusions:** Frontal lobe atrophy in MCI is more extensive than we assumed. In addition, the volume of right MFG_7_1 has the potential to distinguish AD from CN.

Keywords: Alzheimer's disease; mild cognitive impairment; structural magnetic resonance imaging; frontal lobe; subregion cortex

1. Introduction

Alzheimer's disease (AD) is the most common progressive neurodegenerative disease, leading to severe disabilities due to progressive cognitive impairments. With the population aging, the incidence of AD is rising, which imposes a heavy burden on societies. Mild cognitive impairment (MCI) is the prodromal form of AD and is a higher at-risk state for AD [1]. Despite the increase of neuroimaging studies related to AD and MCI over the past decades, the brain structural change underlying the disease has not been fully elucidated.

Gray matter (GM) changes are closely associated with tau pathology in AD patients with abnormal accumulation of amyloids β [2,3]. Therefore, GM atrophy pattern-based morphometric measures have increasingly received attention in AD research [4,5]. As a non-invasive and non-radiative imaging technique, structural magnetic resonance imaging (sMRI) is an alternative method to find neuroimaging evidence for early diagnosis of AD [6]. Data from sMRI of AD suggest that GM atrophy exists in the temporal lobe and prefrontal cortex (PFC) during MCI and further extends to frontal, parietal, and occipital cortexes during the progression from MCI to AD [7–9].

A study found amyloid deposits in the frontal and parietal lobes in patients with mild AD [10]. More amyloid deposits may be associated with faster cortical damage [5]. Therefore, the frontal lobe should be regarded as an important site of AD-associated GM atrophy. The frontal lobe plays an important role in various cognitive processes and is essential for memory, attention, executive function (EF), and self-awareness [11]. Prefrontal cortex (PFC) integrates complex information to form the physiologic constructs of memory, perception, and intricate functions [12], which damage will severely affect executive function (EF) and working memory (WM) [13]. Among the healthy population, larger PFC volume was found to be associated with better execution performance [14]. The middle frontal cortex plays an important role in the maintenance of working memory and response inhibition [15]. The inferior frontal gyrus is pivotal for interference control processes [16]. Moreover, cognitive function is a complex neural process, requiring collaborative effects of different brain regions to operate as a functional brain network. Cognitive decline is closely related to cortical atrophy [17]. However, the relationship between frontal subregions atrophy and cognitive decline in AD or MCI is still unclear.



A reliable and accurate brain partition atlas is crucial for quantitative studies of brain structure in AD. The human Brainnetome (BN-246) atlas [18] is a tractography-based and cross-validated atlas with fine delineation of brain regions and precise boundary localization, containing information on both anatomical and functional connections. Using voxel-based morphometry (VBM), Long *et al.* [4] indicated that the BN-246 atlas is superior to other widely used atlases in distinguishing patients with MCI from cognitively normals (CN). Several studies used the BN-246 atlas to identify the connection between different parts of the cerebral cortex and diseases [4,19,20].

However, the pattern of atrophy in frontal brain regions based on the BNA-246 atlas and its relationship with the cognitive impairments in MCI and AD has not been extensively investigated. We hypothesized that: (1) The atrophy trajectory of the frontal lobe in AD is different from previous studies. (2) The volume of some subregions has a better diagnostic ability to distinguish AD from CN. (3) There is a correlation between certain subregions' volume and cognitive impairment. This study aimed to determine the trajectory of atrophy in frontal subregions and to find which subregion can better differentiate between groups.

2. Material and Methods

2.1 Participants

The data used in this study is from AD Neuroimaging Initiative (ADNI; <http://adni.loni.usc.edu/>). Launched in 2003, ADNI's main goal is to combine serial MRI, positron emission tomography (PET), neuropsychological assessments, and neuroimaging to monitor disease progression in MCI and AD. We included 150 cognitively normals (CN), 187 MCI cases, and 97 AD cases from ADNI-1. The following data for each participant were obtained: T1-weighted MRI, the apolipoprotein E (APOE) genotyping data, and clinical information of patients including age, gender, years of education, Mini-Mental State Examination (MMSE), Alzheimer's Disease Assessment Scale-Cognitive (ADAS-cog) 13, and the Clinical Dementia Rating (CDR) score. MMSE and ADAS-cog have been widely used to assess cognitive function in dementia [21,22], or to estimate disease progression and cognitive change [23–25]. The study procedures were approved by the institutional review boards of all participating institutions. Written informed consents of neuropsychological assessment and neuroimaging were obtained from all study participants or their representatives.

The inclusion and exclusion criteria are as follows. CN subjects: MMSE score is between 24 and 30 (inclusive), CDR is 0, with no signs of MCI, dementia, or depression. MCI subjects: MMSE score is between 24 and 30 (inclusive), CDR is 0.5, and there was a report of a subjective memory problem. With no obvious degree of damage in other cognitive areas, activities of daily living are basically maintained without dementia. Patients with AD met

the Alzheimer's Disease and Related Disorders Association (ADRD) criteria for probable AD [26]. All subjects in our study are prohibited or restricted from using psychotropic substances. More details can be found in ADNI (website: <http://adni.loni.usc.edu/>).

MRI data were collected according to a standardized protocol [27]. This protocol included a high-resolution T1-weighted, rapid gradient echo sequence on a 1.5 T scanner. Acquisition parameters of high resolution T1-weighted fast gradient echo sequence for one platform (Siemens Magnetom Sonata syngo MR 2004 A) were as follows: T1 = 1000 ms, TR = 2400 ms, TE = 3.5, flip Angle = 8, FOV = 240 mm, acquisition matrix = 192×192 , 60 slices and slice thickness of 1.2 mm. According to the ADNI protocol, standardization was exerted on the acquisition techniques of the neuroimage sequences for each scanner and model. Post-acquisition correction of neuroimage artifacts, including geometry corrections for gradient nonlinearity and uneven intensity due to non-uniform receiver coil sensitivity or other reasons, was implemented to improve the standardization of the ADNI sites [27].

2.2 MRI Data Preprocessing

All sMRI data were processed with the VBM toolbox (VBM8, c.gaser, Structural Brain Mapping group, Jena University Hospital, Jena, Germany, version 414, <http://dbm.neuro.uni-jena.de/vbm8/>) implemented in Statistical Parametric Mapping software version 8 (SPM8; Wellcome TrustCenter for Neuroimaging, London, UK; <http://www.fil.ion.ucl.ac.uk/spm>). At first, the T1-weighted image was manually repositioned to the anterior commissure. After unifying segmentation in SPM8, MRI images were segmented into the GM, white matter, cerebral spinal fluid, bone, and soft tissue. GM neuroimages were normalized to a population template in Montreal Neurological Institute space with the high-dimensional DARTEL normalization algorithm. The normalized images were modulated with Jacobian matrices to preserve the actual amounts of a tissue class within each voxel. Then, the modulated images were smoothed with an 8-mm full width at half-maximum Gaussian kernel. Each neuroimage was put into non-linear modulation that displayed the absolute amount of brain tissue, corrected for subject headsize in VBM8. The total cranial internal volume (i.e., estimated total intracranial volume (eTIV)) was calculated based on the sum of GM, WM, and CSF volume obtained from the unstandardized segmented image.

The processed sMRI images were utilized to extract the volume. BNA-246 atlas was used for frontal lobe parcellation. The frontal lobe cortex was divided into six regions, including superior frontal gyrus (SFG), middle frontal gyrus (MFG), inferior frontal gyrus (IFG), orbital gyrus (OrG), precentral gyrus (PrG) and paracentral lobule (PCL). Then, they were divided into 34 regions in each hemisphere, the SFG was divided into seven functional sub-

Table 1. Subregions of the frontal lobe from the Brainnetome Atlas.

The names of frontal lobe subregions from Brainnetome Atlas	Anatomical description
Superior frontal gyrus (SFG)	
SFG_L(R)_7_1	A8m, medial area 8
SFG_L(R)_7_2	A8dl, dorsolateral area 8
SFG_L(R)_7_3	A9l, lateral area 9
SFG_L(R)_7_4	A6dl, dorsolateral area 6
SFG_L(R)_7_5	A6m, medial area 6
SFG_L(R)_7_6	A9m, medial area 9
SFG_L(R)_7_7	A10m, medial area 10
Middle frontal gyrus (MFG)	
MFG_L(R)_7_1	A9/46d, dorsal area 9/46
MFG_L(R)_7_2	IFJ, inferior frontal junction
MFG_L(R)_7_3	A46, area 46
MFG_L(R)_7_4	A9/46v, ventral area 9/46
MFG_L(R)_7_5	A8vl, ventrolateral area 8
MFG_L(R)_7_6	A6vl, ventrolateral area 6
MFG_L(R)_7_7	A10l, lateral area10
Inferior frontal gyrus (IFG)	
IFG_L(R)_6_1	A44d, dorsal area 44
IFG_L(R)_6_2	IFS, inferior frontal sulcus
IFG_L(R)_6_3	A45c, caudal area 45
IFG_L(R)_6_4	A45r, rostral area 45
IFG_L(R)_6_5	A44op, opercular area 44
IFG_L(R)_6_6	A44v, ventral area 44
Orbital gyrus (OrG)	
OrG_L(R)_6_1	A14m, medial area 14
OrG_L(R)_6_2	A12/47o, orbital area 12/47
OrG_L(R)_6_3	A11l, lateral area 11
OrG_L(R)_6_4	A11m, medial area 11
OrG_L(R)_6_5	A13, area 13
OrG_L(R)_6_6	A12/47l, lateral area 12/47
Precentral gyrus (PrG)	
PrG_L(R)_6_1	A4hf, area 4 (head and face region)
PrG_L(R)_6_2	A6cdl, caudal dorsolateral area 6
PrG_L(R)_6_3	A4ul, area 4 (upper limb region)
PrG_L(R)_6_4	A4t, area 4 (trunk region)
PrG_L(R)_6_5	A4tl, area 4 (tongue and larynx region)
PrG_L(R)_6_6	A6cvl, caudal ventrolateral area 6
Paracentral lobule (PCL)	
PCL_L(R)_2_1	A1/2/3ll, area1/2/3 (lower limb region)
PCL_L(R)_2_2	A4ll, area 4 (lower limb region)

Abbreviations: The names of frontal lobe regions and their corresponding anatomical descriptions are from the Brainnetome Atlas [18]; SFG_L(R)_7_1, SFG_7_1 in the left hemisphere or SFG_7_1 in the right hemisphere; MFG_L(R)_7_1, MFG_7_1 in the left hemisphere or in the right hemisphere; IFG_L(R)_6_1, IFG_6_1 in the left hemisphere or in the right hemisphere; OrG_L(R)_6_1, OrG_6_1 in the left hemisphere or in the right hemisphere; PrG_L(R)_6_1, PrG_6_1 in the left hemisphere or in the right hemisphere; PCL_L(R)_2_1, PCL_2_1 in the left hemisphere or in the right hemisphere.

regions, the MFG was divided into seven functional subregions, the IFG was divided into six functional subregions, the OrG was divided into six functional subregions, the PrG was divided into six functional subregions, and the PCL was divided into two functional subregions (Table 1, Ref. [18]).

RESTplus software package (<http://www.restfmri.net>) was used to extract gray matter volume.

Table 2. Demographics and disease-related characteristics of subjects with CN, MCI, and AD.

	CN (n = 150)	MCI (n = 187)	AD (n = 97)	p-value			
				CN vs MCI	MCI vs AD	AD vs CN	CN vs AD
Age, y (mean ± SD)	76.0 ± 4.9	75.1 ± 6.9	75.0 ± 7.3	0.347	0.395	0.576	1
Gender (male/female)	77/73	121/66	49/48	$\chi^2 = 8.154, p = 0.017$	0.015	0.022	1
Education (year)	16.0 ± 2.8	15.8 ± 2.9	14.8 ± 2.9	0.007	1	0.008	0.026
APOE4 (Carriers#/no carriers)	43/107	103/84	67/20	$\chi^2 = 54.62, p < 0.001$	<0.001	<0.001	0.016
MMSE	29.2 ± 1.0	26.8 ± 2.1	23.1 ± 1.9	<0.001	<0.001	<0.001	<0.001
CDR	0 (150)	0.5 (186)	1 (97)	$\chi^2 = 624, p < 0.001$	<0.001	<0.001	<0.001
ADAS-cog 13	5.8 ± 2.8	11.4 ± 4.6	19.1 ± 6.2	<0.001	<0.001	<0.001	<0.001

Abbreviations: “#”, One or two copies of $\epsilon 4$. Education, MMSE, and ADAS-cog 13 were expressed as mean ± SD. CN, cognitively normals; MCI, mild cognitive impairment; AD, Alzheimer’s disease; APOE, apolipoprotein E gene; MMSE, Mini-Mental State Examination; CDR, Clinical Dementia Rating; ADAS-cog, Alzheimer’s Disease Assessment Scale-Cognitive Behavior section.

2.3 Statistical Analysis

Statistical analysis was performed using Statistical Package for Social Sciences software IBM SPSS 28.0 (IBM Corp., Armonk, NY, USA). Data with normal distribution are expressed as mean ± standard deviation. All the statistical tests were two-tailed. Qualitative demographic variables were compared using Chi-square test. Quantitative demographic variables were evaluated using ANOVA. Statistically differences based on ANOVA ($p < 0.05$) were further explored using Bonferroni post hoc analysis when the variances were homogeneous and Dunnett’s T3 post hoc analysis when the variances were heterogeneous. Covariance (ANCOVA) analysis was used to compare the volume differences in frontal lobe regions and subregions with estimated total intracranial volume (eTIV), age, gender, and years of education as covariates. Uncorrected p values were corrected using the false discovery rate (FDR). We also use the receiver operating characteristic (ROC) curve to determine which functional subregion had a better diagnostic ability to differentiate between the groups. Area under the curve (AUC) was calculated and used as a differentiating indicator. p values of less than 0.05 were considered statistically significant. Partial correlation analysis was used to evaluate the relationship between volumetric measurement and cognitive score, with eTIV, age, gender, APOE, and years of education as covariates.

3. Result

3.1 Demographic Data

Table 2 shows the age, gender, education, APOE4 genotype, and scores of MMSE, CDR and ADAS-cog 13. There were no differences in age between groups. The male proportion was higher in the MCI than in CN ($p = 0.015$) and AD ($p = 0.022$) groups. Education level was lower in the AD group than in MCI ($p = 0.008$) and CN ($p = 0.026$). There were significant differences between the groups in APOE $\epsilon 4$ status and MMSE, CDR, and ADAS-cog scores ($p < 0.001$ for all).

3.2 Comparisons Frontal Regions and Subregions Volume between Three Groups

We measured differences in frontal regions and sub-region volumes between the groups using ANCOVA with age, gender, years of education, and eTIV as covariates. The results are shown in Table 3. We found that the volume of SFG, MFG, IFG, and PrG decreased in a stepwise manner in CN, MCI, and AD groups. Compared with the CN group, the volume of most subregions of SFG, MFG, IFG, and OrG was decreased in the MCI group. In addition, right PrG_6_2 and left PrG_6_6 atrophy were evidence.

3.3 Classification Ability of the Volume of Subregions

The AUC values for the three groups are summarized in **Supplementary Table 1**. All p values were < 0.05 . Among subregions of the frontal lobe, the right MFG_7_1 was the best one for distinguishing AD from CN, with an AUC value of 0.7 (Fig. 1). The position of the right MFG_7_1 in the brain is shown in Fig. 2.

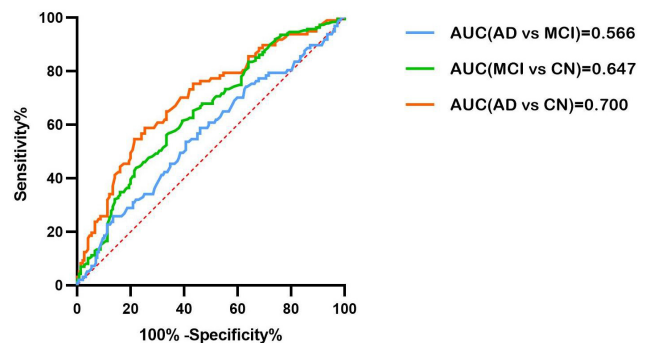


Fig. 1. The ROC curve of the right MFG_7_1 volume in differentiating between AD and MCI (blue), MCI and CN (green), and AD and CN (red). AUC, area under the curve; ROC, receiver operating characteristic; MFG, Middle frontal gyrus; AD, Alzheimer’s disease; MCI, mild cognitive impairment.

Table 3. Comparison of brain region volume in the frontal lobe between the CN, MCI, and AD groups based on the BNA-246 atlas.

Brain regions or subregions	CN (n = 150)	MCI (n = 187)	AD (n = 97)	p-value		
				MCI vs CN	AD vs CN	MCI vs AD
SFG	0.40 ± 0.05	0.39 ± 0.05	0.38 ± 0.05	0.014*	<0.001**	0.073
SFG_L_7_1	0.43 ± 0.07	0.42 ± 0.07	0.41 ± 0.07	0.443	0.025*	0.433
SFG_R_7_1	0.43 ± 0.07	0.41 ± 0.07	0.40 ± 0.07	0.23	<0.001**	0.036*
SFG_L_7_2	0.42 ± 0.08	0.40 ± 0.08	0.38 ± 0.08	0.034*	<0.001**	0.056
SFG_R_7_2	0.43 ± 0.08	0.40 ± 0.08	0.39 ± 0.08	0.05	<0.001**	0.202
SFG_L_7_3	0.30 ± 0.06	0.28 ± 0.07	0.27 ± 0.08	0.198	0.004*	0.261
SFG_R_7_3	0.32 ± 0.07	0.30 ± 0.07	0.30 ± 0.06	0.161	0.012*	0.571
SFG_L_7_4	0.38 ± 0.09	0.36 ± 0.08	0.34 ± 0.09	0.183	0.002*	0.176
SFG_R_7_4	0.38 ± 0.09	0.35 ± 0.07	0.34 ± 0.08	0.018*	0.002*	0.799
SFG_L_7_5	0.45 ± 0.07	0.44 ± 0.07	0.43 ± 0.08	0.284	0.020*	0.531
SFG_R_7_5	0.43 ± 0.07	0.42 ± 0.07	0.41 ± 0.07	0.301	0.025*	0.569
SFG_L_7_6	0.47 ± 0.06	0.45 ± 0.07	0.45 ± 0.06	0.095	0.002*	0.252
SFG_R_7_6	0.45 ± 0.06	0.43 ± 0.06	0.42 ± 0.06	0.038*	<0.001**	0.093
SFG_L_7_7	0.39 ± 0.05	0.37 ± 0.06	0.37 ± 0.06	0.024*	0.001*	0.465
SFG_R_7_7	0.39 ± 0.05	0.37 ± 0.06	0.37 ± 0.05	0.014*	0.001*	0.382
MFG	0.32 ± 0.04	0.30 ± 0.04	0.29 ± 0.04	<0.001**	<0.001**	0.304
MFG_L_7_1	0.40 ± 0.06	0.38 ± 0.06	0.36 ± 0.07	0.003*	<0.001**	0.020*
MFG_R_7_1	0.46 ± 0.06	0.42 ± 0.07	0.41 ± 0.07	<0.001**	<0.001**	0.092
MFG_L_7_2	0.43 ± 0.06	0.41 ± 0.06	0.40 ± 0.07	0.036*	<0.001**	0.076
MFG_R_7_2	0.44 ± 0.08	0.43 ± 0.07	0.40 ± 0.08	0.297	<0.001**	0.009*
MFG_L_7_3	0.35 ± 0.05	0.32 ± 0.06	0.31 ± 0.06	0.002*	<0.001**	0.402
MFG_R_7_3	0.39 ± 0.06	0.36 ± 0.07	0.35 ± 0.07	<0.001**	<0.001**	0.108
MFG_L_7_4	0.43 ± 0.06	0.40 ± 0.07	0.40 ± 0.07	0.005*	0.001*	0.956
MFG_R_7_4	0.44 ± 0.07	0.41 ± 0.07	0.39 ± 0.07	0.003*	<0.001**	0.556
MFG_L_7_5	0.40 ± 0.06	0.36 ± 0.06	0.34 ± 0.08	0.009*	<0.001**	0.030*
MFG_R_7_5	0.38 ± 0.08	0.35 ± 0.08	0.33 ± 0.08	0.006*	<0.001**	0.267
MFG_L_7_6	0.42 ± 0.08	0.40 ± 0.09	0.37 ± 0.09	0.094	<0.001**	0.025*
MFG_R_7_6	0.41 ± 0.09	0.389 ± 0.083	0.369 ± 0.090	0.048*	<0.001**	0.245
MFG_L_7_7	0.37 ± 0.07	0.34 ± 0.07	0.34 ± 0.07	0.009*	0.004*	1
MFG_R_7_7	0.41 ± 0.06	0.38 ± 0.07	0.38 ± 0.07	0.022*	0.006*	1
IFG	0.44 ± 0.06	0.41 ± 0.06	0.40 ± 0.06	0.006*	<0.001**	0.018*
IFG_L_6_1	0.49 ± 0.08	0.47 ± 0.09	0.45 ± 0.10	0.092	<0.001**	0.081
IFG_R_6_1	0.47 ± 0.09	0.44 ± 0.09	0.43 ± 0.08	0.016*	<0.001**	0.497
IFG_L_6_2	0.39 ± 0.07	0.35 ± 0.07	0.35 ± 0.08	0.006*	<0.001**	0.073
IFG_R_6_2	0.46 ± 0.09	0.43 ± 0.09	0.44 ± 0.1	0.009*	0.004*	1
IFG_L_6_3	0.39 ± 0.07	0.39 ± 0.08	0.38 ± 0.08	1	0.319	0.926
IFG_R_6_3	0.38 ± 0.09	0.37 ± 0.08	0.36 ± 0.09	0.433	0.051	0.685
IFG_L_6_4	0.38 ± 0.07	0.35 ± 0.08	0.35 ± 0.08	0.018*	0.004*	0.948
IFG_R_6_4	0.42 ± 0.09	0.40 ± 0.08	0.38 ± 0.09	0.616	0.018*	0.238
IFG_L_6_5	0.41 ± 0.05	0.39 ± 0.07	0.38 ± 0.06	0.003*	<0.001**	0.856
IFG_R_6_5	0.48 ± 0.07	0.46 ± 0.06	0.45 ± 0.07	0.037*	0.001*	0.359
IFG_L_6_6	0.48 ± 0.08	0.46 ± 0.08	0.46 ± 0.09	0.136	0.014*	0.647
IFG_R_6_6	0.49 ± 0.10	0.46 ± 0.09	0.44 ± 0.09	0.572	<0.001**	0.014*
OrG	0.57 ± 0.05	0.54 ± 0.06	0.54 ± 0.06	0.002*	<0.001**	0.169
OrG_L_6_1	0.50 ± 0.07	0.47 ± 0.07	0.47 ± 0.07	0.004*	0.004*	1
OrG_R_6_1	0.57 ± 0.07	0.54 ± 0.08	0.52 ± 0.08	<0.001**	<0.001**	0.242
OrG_L_6_2	0.56 ± 0.07	0.54 ± 0.08	0.53 ± 0.08	0.073	0.004*	0.556
OrG_R_6_2	0.52 ± 0.07	0.50 ± 0.07	0.50 ± 0.07	0.136	0.022*	0.872
OrG_L_6_3	0.63 ± 0.07	0.60 ± 0.070	0.59 ± 0.07	0.014*	<0.001**	0.397
OrG_R_6_3	0.62 ± 0.06	0.59 ± 0.07	0.59 ± 0.07	0.022*	0.003*	0.799

Table 4. The correlation of frontal subregion volumes with MMSE and ADAS-cog 13 scores in MCI.

	MMSE		ADAS-cog 13	
	r	p-value	r	p-value
SFG_L_7_1	-0.035	0.641	-0.157	0.034*
SFG_R_7_1	-0.031	0.679	-0.175	0.018*
SFG_L_7_2	0.049	0.514	-0.182	0.014*
SFG_R_7_2	0.021	0.777	-0.184	0.013*
SFG_L_7_3	0.013	0.864	-0.199	0.007*
SFG_R_7_3	-0.035	0.641	-0.203	0.006*
SFG_L_7_4	0.092	0.275	-0.165	0.026*
SFG_R_7_4	0.055	0.463	-0.192	0.009*
SFG_L_7_7	0.021	0.774	-0.17	0.021*
MFG_L_7_1	0.059	0.428	-0.188	0.011*
MFG_R_7_1	0.089	0.232	-0.17	0.022*
MFG_R_7_2	0.033	0.656	-0.156	0.035*
MFG_R_7_3	0.129	0.082	-0.158	0.032*
MFG_R_7_4	0.005	0.944	-0.175	0.018*
MFG_L_7_5	0.079	0.29	-0.168	0.023*
MFG_R_7_5	0.067	0.371	-0.278	<0.001**
MFG_L_7_6	0.07	0.334	-0.201	0.006*
MFG_R_7_6	0.048	0.521	-0.199	0.007*
IFG_R_6_4	0.056	0.449	-0.202	0.006*
OrG_L_6_5	-0.104	0.16	-0.218	0.003*
OrG_R_6_5	0.099	0.184	-0.179	0.015*
ORG_R_6_6	0.059	0.427	-0.184	0.013*
PrG_L_6_2	0.049	0.507	-0.245	<0.001**
PrG_R_6_2	0.103	0.164	-0.257	<0.001**
PRG_R_6_5	0.116	0.119	-0.205	0.005*
PCL_L_2_1	0.021	0.778	-0.183	0.013*

Abbreviations: * $p < 0.05$, ** $p < 0.001$; r, correlation coefficient; Only frontal subregions in the MCI that were statistically related to MMSE or ADAS-cog 13 are displayed.

= -0.351, $p = 0.001$), and right IFG_6_6 ($r = -0.326$, $p = 0.001$) for the ADAS-cog 13.

4. Discussion

In this study, we first compared grey matter volume (GMV) in frontal regions and subregions between AD, MCI, and CN groups. Then, the AUC results demonstrated that the right MFG_7_1 has a satisfactory ability to distinguish between AD and CN. Furthermore, after adjustment for age, gender, years of education, and eTIV, we found that the right IFG_6_1, the left IFG_6_3, the right IFG_6_3, the right IFG_6_5, the right OrG_6_5, and the right OrG_6_6 with ADAS-cog 13 score and slightly correlated with MMSE score in patients with AD.

In our study, widespread cortical atrophy was found in the bilateral frontal lobes in patients with MCI, which was exacerbated by disease progression [7–9]. The right dorsal area 9/46 (right MFG_7_1) showed a more severe atrophy and its volume is the best one to distinguish AD patients from CN. In addition, PrG subregion atrophy was found

Table 5. Correlation of the subregions volume of frontal lobe measures with MMSE and ADAS-cog 13 scores in AD.

	MMSE		ADAS-cog 13	
	r	p-value	r	p-value
SFG_L_7_2	0.218	0.035*	-0.23	0.027*
SFG_L_7_3	0.1119	0.256	-0.21	0.043*
SFG_R_7_6	0.216	0.038*	-0.149	0.155
MFG_L_7_1	0.183	0.078	-0.222	0.033*
MFG_R_7_1	0.236	0.023*	-0.206	0.047*
MFG_R_7_3	0.266	0.01*	-0.212	0.042*
MFG_L_7_4	0.172	0.1	-0.025	0.049*
MFG_L_7_7	0.202	0.052	-0.239	0.021*
IFG_L_6_1	0.175	0.094	-0.289	0.005*
IFG_R_6_1	0.094	0.368	-0.321	0.002*
IFG_L_6_2	0.062	0.555	-0.308	0.003*
IFG_L_6_3	-0.024	0.822	-0.252	0.015*
IFG_R_6_3	0.216	0.038*	-0.309	0.003*
IFG_L_6_4	0.124	0.238	-0.28	0.007*
IFG_L_6_5	0.169	0.105	-0.254	0.014*
IFG_R_6_5	0.299	0.004*	-0.333	0.001*
OrG_L_6_1	0.162	0.121	-0.258	0.013*
OrG_R_6_1	0.147	0.158	-0.273	0.008*
OrG_L_6_2	0.19	0.068	-0.226	0.03*
OrG_R_6_2	0.159	0.1229	-0.228	0.028*
OrG_L_6_4	0.163	0.118	-0.221	0.033*
OrG_R_6_4	0.089	0.394	-0.276	0.007*
OrG_L_6_5	0.138	0.186	-0.295	0.004*
OrG_R_6_5	0.212	0.042*	-0.351	<0.001**
OrG_L_6_6	0.183	0.079	-0.282	0.006*
OrG_R_6_6	0.283	0.006*	-0.326	0.001*

Abbreviations: * $p < 0.05$, ** $p < 0.001$; r, correlation coefficient; Only frontal subregions that were statistically related to MMSE or ADAS-cog 13 scores are displayed.

in patients with MCI. Machine learning has suggested that the precentral gyrus is one of several regions affected by AD [28]. However, no studies reported decreased PrG volume in MCI patients through voxel-based morphometry. Compared with previous studies of MCI [7,9], our results suggested more extensive frontal cortical deficits. Using magnetic resonance elastography (MRE), Lucy *et al.* [29] identified stiffness deficits in the frontal operculum and PrG. PrG_6_6 corresponds to the caudal ventrolateral area 6 [18], and controls muscle contraction and speech [30]. Moreover, it may control eye blinking [31], and an abnormally high eye blink rate may be characteristic of subjects with MCI [32].

The frontal cortex is a heterogeneous region with multiple functional subdivisions, and damage to different subdivisions can impair different cognitive functions, including memory, language, response inhibition, and cognitive flexibility. ADAS-cog 13, whose scores range from 0 to 85, with higher scores indicating more severe cognitive impairment. MMSE, the score ranges from 0 to 30, with

lower scores indicating more severe cognitive impairment. Among patients with AD, the volume of these subregions was more robustly correlated with ADAS-cog 13 than with the MMSE score. The reason may be the greater involvement of memory, language, and orientation in the ADAS-cog 13 than in the MMSE. Due to the ceiling effect, MMSE may lack sensitivity to early cognitive impairment, which may lead to the absence of any correlations between subregion volumes and MMSE score in MCI. Despite our findings, Han *et al.* [33] reported that volume reduction in the left inferior frontal gyrus is related to the severity of symptoms in MCI. Differences in the MCI groups may warrant this discrepancy between the studies. Han *et al.* [33] recruited amnesic MCI patients, whereas MCI includes more heterogeneous groups of patients [34].

Broca's area is essential for speech production [35]. It has been divided into BA 44 and BA 45 [36], usually in the left hemisphere. However, the right BA 44 also plays an important role in successful language. The right BA 44 is also involved in language processing in both visual and auditory ways [37]. Moreover, BA 44 is considered the core area of syntax processing [38]. There is growing evidence that cross-hemispheric communication is also important for syntactic learning and processing [39,40]. Chen L *et al.* [40] suggested that right BA 44 may transfer information to left BA44 for promoting syntactic operations. In our study, the BA 44 was further subdivided into ventral (IFG_6_1), dorsal (IFG_6_6), and operculum parts (IFG_6_5) subregions [41]. BA 45 was subdivided into caudal (IFG_6_3) and rostral (IFG_6_4) areas. Molnar-Szakacs *et al.* [42] reported that the dorsal part of area 45 is active during observation and imitation, whereas the ventral part is active just during imitation, but not during observation. In this study, cognitive function was correlated with right IFG_6_1 and right IFG_6_3 volumes, but not with IFG_6_6 and IFG_6_4 volumes, which warrants further parcellation within the BA 44 and BA 45.

The right BA 44 might function beyond phonological processing. The operculum (IFG_6_5) is crucial for successful response inhibition and task-switching in the stop-signal task [43,44]. The inability to maintain directed attention in the presence of interfering stimuli may be the mechanism underlying frontal lobe memory deficit [45]. Meanwhile, the right IFG_6_5 is involved in integrating exteroceptive and interoceptive signals, which are necessary for interoceptive awareness. The defect may be responsible for the lack of insight, which is a frequent symptom of dementia [18,46]. Inferior frontal sulcus areas of the left hemisphere (left IFG_6_2) are associated with language and working memory [47].

The right IFG and its connections with the striatum may be the basis of cognitive control, whereas the right ventrolateral prefrontal cortex (VLPFC) is a critical area in control [16,44]. VLPFC is a component of the ventral attention (VANet), dorsal attention (DANet), and salience

(SNet) networks. These brain network patterns are important for cognitive flexibility [48,49]. Cognitive flexibility, also known as behavioral flexibility, relies on both inhibitory control and WM. Transient inactivation of the right VLPFC, including right IFG_6_3, right IFG_6_4, right OrG_6_2, and right OrG_6_6 subregions, impairs audiovisual working memory performance [50]. In this study, the right OrG_6_5 and OrG_6_6 were correlated with cognitive function. OrG_6_5 is a part of the orbitofrontal cortex (OFC), whose lesions usually affect flexible cognitive processes such as learning, recognition, and drive response [51,52]. Therefore, the impaired function of these areas can affect different aspects of cognition.

5. Limitations and Further Considerations

Although MMSE items cover several cognitive domains, they are unlikely to identify more subtle cognitive changes related to frontal subregions, as MMSE is a global scale of cognitive impairment. The most important disadvantage of MMSE is low sensitivity to MCI. More sensitive and precise measures of frontal lobe function, such as verbal fluency test and false memory test [53,54], are recommended for future studies. It has been shown that some brain networks are disrupted in AD [55]. Cognitive function depends on the normal function of multiple regions in the brain network. Cognitive impairment is also associated with abnormal connectivity between different brain regions [56]. Changes in the functional connectivity of the intrinsic network can be detected by resting state fMRI. Whether there is a compensatory mechanism between brain regions can be explored by task-state fMRI. The combination of multimodal imaging, such as structural and functional MRI, can provide a great deal of information to expand our understanding of the mechanisms of brain changes in AD. Furthermore, the BNA-246 atlas we used in this study was developed in the Chinese population, and the results of this study need to be further verified among Chinese patients with MCI and AD.

6. Conclusions

(1) There is atrophy in the frontal superior frontal gyrus, middle frontal gyrus, inferior frontal gyrus, orbital gyrus and precentral gyrus in MCI. Dividing the frontal lobe into 34 subregions can more accurately and objectively analyze the structural changes of the frontal lobe in MCI and AD patients. (2) The 9/46 area of the middle frontal gyrus is an important part of the structural changes of the frontal lobe in AD patients, which helps to promote the exploration of the pathological mechanism of the frontal lobe in AD patients. (3) Atrophy of certain frontal subregion cortex is associated with cognitive dysfunction in AD patients.

Availability of Data and Materials

The raw data supporting the conclusions of this manuscript will be made available by the authors, without undue reservation, to any qualified researcher.

Author Contributions

All authors contributed significantly to this research and preparation of the manuscript. Conceived and designed the experiments—CS, XD, WY. Performed the experiments and analyzed the data—CS, HD, DR. All authors have been involved in the drafting, critical revision, and final approval of the manuscript for publication. All authors agree to be accountable for all aspects of the work in ensuring that questions related to the accuracy or integrity of any part of the work are appropriately investigated and resolved. All authors read and approved the final manuscript.

Ethics Approval and Consent to Participate

The study has been approved by Medical Ethics Committee of Affiliated Hospital of North Sichuan Medical College with the IRB number (2022ER452-1). The patient consent form was waived which was approved by IRB.

Acknowledgment

We thank all of the study participants and their families that participated in the neuroimaging research. Data used in preparation of this article were obtained from the Alzheimer's Disease Neuroimaging Initiative (ADNI) database (<http://adni.loni.usc.edu>). As such, the investigators within the ADNI contributed to the design and implementation of ADNI and/or provided data but did not participate in analysis or writing of this report. We also appreciate their contributions. A complete listing of ADNI investigators can be found at http://adni.loni.usc.edu/wp-content/uploads/how_to_apply/ADNI_Acknowledgement_List.pdf.

Funding

This research received no external funding.

Conflict of Interest

The authors declare no conflict of interest.

Supplementary Material

Supplementary material associated with this article can be found, in the online version, at <https://doi.org/10.31083/j.jin2204099>.

References

- [1] Petersen RC, Doody R, Kurz A, Mohs RC, Morris JC, Rabins PV, *et al.* Current concepts in mild cognitive impairment. *Archives of Neurology*. 2001; 58: 1985–1992.
- [2] Pelkmans W, Ossenkoppele R, Dicks E, Strandberg O, Barkhof F, Tijms BM, *et al.* Tau-related grey matter network breakdown across the Alzheimer's disease continuum. *Alzheimer's Research & Therapy*. 2021; 13: 138.
- [3] Montembeault M, Brambati SM, Lamari F, Michon A, Samri D, Epelbaum S, *et al.* Atrophy, metabolism and cognition in the posterior cortical atrophy spectrum based on Alzheimer's disease cerebrospinal fluid biomarkers. *NeuroImage. Clinical*. 2018; 20: 1018–1025.
- [4] Long Z, Huang J, Li B, Li Z, Li Z, Chen H, *et al.* A Comparative Atlas-Based Recognition of Mild Cognitive Impairment With Voxel-Based Morphometry. *Frontiers in Neuroscience*. 2018; 12: 916.
- [5] Contador J, Pérez-Millán A, Tort-Merino A, Balasa M, Falgàs N, Olives J, *et al.* Longitudinal brain atrophy and CSF biomarkers in early-onset Alzheimer's disease. *NeuroImage. Clinical*. 2021; 32: 102804.
- [6] Blamire AM. MR approaches in neurodegenerative disorders. *Progress in Nuclear Magnetic Resonance Spectroscopy*. 2018; 108: 1–16.
- [7] Karas GB, Scheltens P, Rombouts SARB, Visser PJ, van Schijndel RA, Fox NC, *et al.* Global and local gray matter loss in mild cognitive impairment and Alzheimer's disease. *NeuroImage*. 2004; 23: 708–716.
- [8] Kinkingnéhun S, Sarazin M, Lehericy S, Guichart-Gomez E, Hergueta T, Dubois B. VBM anticipates the rate of progression of Alzheimer disease: a 3-year longitudinal study. *Neurology*. 2008; 70: 2201–2211.
- [9] Hämäläinen A, Tervo S, Grau-Olivares M, Niskanen E, Pennanen C, Huuskonen J, *et al.* Voxel-based morphometry to detect brain atrophy in progressive mild cognitive impairment. *NeuroImage*. 2007; 37: 1122–1131.
- [10] Klunk WE, Engler H, Nordberg A, Wang Y, Blomqvist G, Holt DP, *et al.* Imaging brain amyloid in Alzheimer's disease with Pittsburgh Compound-B. *Annals of Neurology*. 2004; 55: 306–319.
- [11] Chayer C, Freedman M. Frontal lobe functions. *Current Neurology and Neuroscience Reports*. 2001; 1: 547–552.
- [12] Masterman DL, Cummings JL. Frontal-subcortical circuits: the anatomic basis of executive, social and motivated behaviors. *Journal of Psychopharmacology (Oxford, England)*. 1997; 11: 107–114.
- [13] Garcia-Alvarez L, Gomar JJ, Sousa A, Garcia-Portilla MP, Goldberg TE. Breadth and depth of working memory and executive function compromises in mild cognitive impairment and their relationships to frontal lobe morphometry and functional competence. *Alzheimer's & Dementia (Amsterdam, Netherlands)*. 2019; 11: 170–179.
- [14] Yuan P, Raz N. Prefrontal cortex and executive functions in healthy adults: a meta-analysis of structural neuroimaging studies. *Neuroscience and Biobehavioral Reviews*. 2014; 42: 180–192.
- [15] Hester R, Murphy K, Garavan H. Beyond common resources: the cortical basis for resolving task interference. *NeuroImage*. 2004; 23: 202–212.
- [16] Puglisi G, Howells H, Sciortino T, Leonetti A, Rossi M, Conti Nibali M, *et al.* Frontal pathways in cognitive control: direct evidence from intraoperative stimulation and diffusion tractography. *Brain*. 2019; 142: 2451–2465.
- [17] Fox NC, Scahill RI, Crum WR, Rossor MN. Correlation between rates of brain atrophy and cognitive decline in AD. *Neurology*. 1999; 52: 1687–1689.
- [18] Fan L, Li H, Zhuo J, Zhang Y, Wang J, Chen L, *et al.* The Human Brainnetome Atlas: A New Brain Atlas Based on Connectional Architecture. *Cerebral Cortex (New York, N.Y.: 1991)*. 2016; 26: 3508–3526.
- [19] Wang H, McGonigal A, Zhang K, Guo Q, Zhang B, Wang X, *et al.* Semiologic subgroups of insulo-opercular seizures based on connectional architecture atlas. *Epilepsia*. 2020; 61: 984–994.

- [20] Shi W, Fan L, Jiang T. Developing Neuroimaging Biomarker for Brain Diseases with a Machine Learning Framework and the Brainnetome Atlas. *Neuroscience Bulletin*. 2021; 37: 1523–1525.
- [21] Fortier-Brochu E, Morin CM. Cognitive impairment in individuals with insomnia: clinical significance and correlates. *Sleep*. 2014; 37: 1787–1798.
- [22] Lövdén M, Fratiglioni L, Glymour MM, Lindenberg U, Tucker-Drob EM. Education and Cognitive Functioning Across the Life Span. *Psychological Science in the Public Interest*. 2020; 21: 6–41.
- [23] Darmanthé N, Tabatabaei-Jafari H, Cherbuin N, Alzheimer's Disease Neuroimaging Initiative. Combination of Plasma Neurofilament Light Chain and Mini-Mental State Examination Score Predicts Progression from Mild Cognitive Impairment to Alzheimer's Disease within 5 Years. *Journal of Alzheimer's Disease*. 2021; 82: 951–964.
- [24] Arevalo-Rodriguez I, Smailagic N, Roqué-Figuls M, Ciapponi A, Sanchez-Perez E, Giannakou A, *et al.* Mini-Mental State Examination (MMSE) for the early detection of dementia in people with mild cognitive impairment (MCI). *The Cochrane Database of Systematic Reviews*. 2021; 7: CD010783.
- [25] Lin C, Chen C, Tom SE, Kuo S, Alzheimer's Disease Neuroimaging Initiative. Cerebellar Volume Is Associated with Cognitive Decline in Mild Cognitive Impairment: Results from ADNI. *Cerebellum* (London, England). 2020; 19: 217–225.
- [26] Dubois B, Feldman HH, Jacova C, Dekosky ST, Barberger-Gateau P, Cummings J, *et al.* Research criteria for the diagnosis of Alzheimer's disease: revising the NINCDS-ADRDA criteria. *The Lancet. Neurology*. 2007; 6: 734–746.
- [27] Jack CR, Bernstein MA, Fox NC, Thompson P, Alexander G, Harvey D, *et al.* The Alzheimer's Disease Neuroimaging Initiative (ADNI): MRI methods. *Journal of Magnetic Resonance Imaging: JMRI*. 2008; 27: 685–691.
- [28] Zhang Y, Dong Z, Phillips P, Wang S, Ji G, Yang J, *et al.* Detection of subjects and brain regions related to Alzheimer's disease using 3D MRI scans based on eigenbrain and machine learning. *Frontiers in Computational Neuroscience*. 2015; 9: 66.
- [29] Hiscox LV, Johnson CL, McGarry MDJ, Marshall H, Ritchie CW, van Beek EJR, *et al.* Mechanical property alterations across the cerebral cortex due to Alzheimer's disease. *Brain Communications*. 2020; 2: fcz049.
- [30] Trevisi G, Eickhoff SB, Chowdhury F, Jha A, Rodionov R, Nowell M, *et al.* Probabilistic electrical stimulation mapping of human medial frontal cortex. *Cortex; a Journal Devoted to the Study of the Nervous System and Behavior*. 2018; 109: 336–346.
- [31] Kato M, Miyauchi S. Human precentral cortical activation patterns during saccade tasks: an fMRI comparison with activation during intentional eyeblink tasks. *NeuroImage*. 2003; 19: 1260–1272.
- [32] D'Antonio F, Bartolo MID, Ferrazzano G, Monti MS, Imbriano L, Trebbastoni A, *et al.* Blink Rate Study in Patients with Alzheimer's Disease, Mild Cognitive Impairment and Subjective Cognitive Decline. *Current Alzheimer Research*. 2021; 18: 1104–1110.
- [33] Han Y, Lui S, Kuang W, Lang Q, Zou L, Jia J. Anatomical and functional deficits in patients with amnesic mild cognitive impairment. *PLoS ONE*. 2012; 7: e28664.
- [34] Bell-McGinty S, Lopez OL, Meltzer CC, Scanlon JM, Whyte EM, Dekosky ST, *et al.* Differential cortical atrophy in subgroups of mild cognitive impairment. *Archives of Neurology*. 2005; 62: 1393–1397.
- [35] Keller SS, Crow T, Foundas A, Amunts K, Roberts N. Broca's area: nomenclature, anatomy, typology and asymmetry. *Brain Lang*. 2009 Apr; 109(1):29–48
- [36] Amunts K, Schleicher A, Bürgel U, Mohlberg H, Uylings HB, Zilles K. Broca's region revisited: cytoarchitecture and intersubject variability. *The Journal of Comparative Neurology*. 1999; 412: 319–341.
- [37] Baumgaertner A, Hartwigsen G, Roman Siebner H. Right-hemispheric processing of non-linguistic word features: implications for mapping language recovery after stroke. *Human Brain Mapping*. 2013; 34: 1293–1305.
- [38] Goucha T, Friederici AD. The language skeleton after dissecting meaning: A functional segregation within Broca's Area. *NeuroImage*. 2015; 114: 294–302.
- [39] Hagoort P. The neurobiology of language beyond single-word processing. *Science (New York, N.Y.)*. 2019; 366: 55–58.
- [40] Chen L, Wu J, Hartwigsen G, Li Z, Wang P, Feng L. The role of a critical left fronto-temporal network with its right-hemispheric homologue in syntactic learning based on word category information. *Journal of Neurolinguistics*. 2021; 58: 100977.
- [41] Amunts K, Lenzen M, Friederici AD, Schleicher A, Morosan P, Palomero-Gallagher N, *et al.* Broca's region: novel organizational principles and multiple receptor mapping. *PLoS Biology*. 2010; 8: e1000489.
- [42] Molnar-Szakacs I, Iacoboni M, Koski L, Mazziotta JC. Functional segregation within pars opercularis of the inferior frontal gyrus: evidence from fMRI studies of imitation and action observation. *Cerebral Cortex (New York, N.Y.: 1991)*. 2005; 15: 986–994.
- [43] Aron AR, Monsell S, Sahakian BJ, Robbins TW. A componential analysis of task-switching deficits associated with lesions of left and right frontal cortex. *Brain: a Journal of Neurology*. 2004; 127: 1561–1573.
- [44] Aron AR, Robbins TW, Poldrack RA. Inhibition and the right inferior frontal cortex. *Trends in Cognitive Sciences*. 2004; 8: 170–177.
- [45] Stuss DT, Benson DF. The frontal lobes revisited: The frontal lobes and control of cognition and memory. 1st edn. *Psychology Press: New York*. 1987.
- [46] Blefari ML, Martuzzi R, Salomon R, Bello-Ruiz J, Herbelin B, Serino A, *et al.* Bilateral Rolandic operculum processing underlying heartbeat awareness reflects changes in bodily self-consciousness. *The European Journal of Neuroscience*. 2017; 45: 1300–1312.
- [47] Ruland SH, Palomero-Gallagher N, Hoffstaedter F, Eickhoff SB, Mohlberg H, Amunts K. The inferior frontal sulcus: Cortical segregation, molecular architecture and function. *Cortex; a Journal Devoted to the Study of the Nervous System and Behavior*. 2022; 153: 235–256.
- [48] Trambaiolli LR, Peng X, Lehman JF, Linn G, Russ BE, Schroeder CE, *et al.* Anatomical and functional connectivity support the existence of a salience network node within the caudal ventrolateral prefrontal cortex. *ELife*. 2022; 11: e76334.
- [49] Dajani DR, Uddin LQ. Demystifying cognitive flexibility: Implications for clinical and developmental neuroscience. *Trends in Neurosciences*. 2015; 38: 571–578.
- [50] Plakke B, Hwang J, Romanski LM. Inactivation of Primate Prefrontal Cortex Impairs Auditory and Audiovisual Working Memory. *The Journal of Neuroscience: the Official Journal of the Society for Neuroscience*. 2015; 35: 9666–9675.
- [51] Wikenheiser AM, Schoenbaum G. Over the river, through the woods: cognitive maps in the hippocampus and orbitofrontal cortex. *Nature Reviews Neuroscience*. 2016; 17: 513–523.
- [52] Rolls ET, Grabenhorst F. The orbitofrontal cortex and beyond: from affect to decision-making. *Progress in Neurobiology*. 2008; 86: 216–244.
- [53] Murphy KJ, West R, Armilio ML, Craik FIM, Stuss DT. Word-list-learning performance in younger and older adults: intra-individual performance variability and false memory. *Neuropsychol*

chology, Development, and Cognition. Section B, Aging, Neuropsychology and Cognition. 2007; 14: 70–94.

- [54] Kwak S, Shin SA, Ko H, Kim H, Oh DJ, Youn JH, *et al.* A Comparison Between the Performances of Verbal and Nonverbal Fluency Tests in Discriminating Between Mild Cognitive Impairments and Alzheimer's Disease Patients and Their Brain Morphological Correlates. *Dementia and Neurocognitive Disorders*. 2022; 21: 17–29.
- [55] Bozzali M, Padovani A, Caltagirone C, Borroni B. Regional grey matter loss and brain disconnection across Alzheimer disease evolution. *Current Medicinal Chemistry*. 2011; 18: 2452–2458.
- [56] Liang P, Wang Z, Yang Y, Jia X, Li K. Functional disconnection and compensation in mild cognitive impairment: evidence from DLPFC connectivity using resting-state fMRI. *PLoS ONE*. 2011; 6: e22153.